Magnetic ordering and electrical transport in $R_{0.5}Sr_{0.5}MnO_{3-\gamma}$ (R = Sm, Eu, Gd, Tb, Dy, Y, Bi) compounds



1997 J. Phys.: Condens. Matter 9 7455

(http://iopscience.iop.org/0953-8984/9/35/018)

J. Phys.: Condens. Matter **9** (1997) 7455–7461. Printed in the UK PII: S0953-8984(97)82144-3

# Magnetic ordering and electrical transport in $R_{0.5}Sr_{0.5}MnO_{3-\gamma}$ (R = Sm, Eu, Gd, Tb, Dy, Y, Bi) compounds

N V Kasper†, I O Troyanchuk†, A N Chobot†, H Szymczak‡ and J Fink-Finowicki‡

† Institute of Physics of Solids and Semiconductors, Academy of Sciences of Belarus, P Brovki 17, 220072 Minsk, Belarus

‡ Institute of Physics, Polish Academy of Sciences, al. Lotnikow 32/46, 02-668 Warsaw, Poland

Received 25 February 1997, in final form 1 July 1997

**Abstract.** Magnetic and electrical properties of the $R_{0.5}Sr_{0.5}MnO_{3-\gamma}$ (R = Sm, Eu, Gd, Tb, Dy, Y) compounds have been studied. All the samples have the same pseudo-cubic perovskite structure with small unit-cell distortions. The decreasing of rare-earth ion radii leads to destruction of both the long-range ferromagnetic and charge order and stabilizes a spin-glass-like state. The $Sm_{0.5}Sr_{0.5}MnO_{3-\gamma}$ ferromagnet compound exhibits a peak of resistivity and anomalous behaviour of elastic properties at around $T_C = 125$ K whereas the resistivity and magnetoresistance of the $R_{0.5}Sr_{0.5}MnO_{3-\gamma}$ (R = Eu, Gd, Tb) spin glass increase gradually with decreasing temperature.

## 1. Introduction

The observation of colossal magnetoresistance at the Curie temperature of $La_{1-x}A_xMnO_3$ (A = Sr, Ca, Pb, Ba) has attracted considerable attention [1, 2]. Recently, it has been shown that another type of colossal magnetoresistance in the $R_{1-x}A_xMnO_3$ (R = rare-earth ion; A = Ca, Sr) systems can arise from 'melting' the ordered state of $Mn^{3+}$ and $Mn^{4+}$ ions in an external magnetic field [3, 4]. The charge-ordered state is found in samples of $La_{0.5}Ca_{0.5}MnO_3$ [5], $Pr_{1-x}Ca_xMnO_3$ ($0.3 \leqslant x < 0.5$) [6], $Pr_{0.5}Sr_{0.5}MnO_3$ [3, 7] and $Nd_{0.5}Sr_{0.5}MnO_3$ [4].

$Pr_{0.5}Sr_{0.5}(Mn^{3+}_{0.5}Mn^{4+}_{0.5})O_3$ has a ferromagnetic transition at 270 K, below which there is a matching change in the resistivity. At 140 K charge ordering occurs with a simultaneous transition into an antiferromagnetic state and a giant increase in resistivity due to localization of the charge carriers. The charge-ordered state is destroyed by applying a sufficiently large external magnetic field. The magnetic-field-induced transition is believed to be of first order and shows a large hysteresis. At low temperature the field-induced transition becomes irreversible. The behaviour of $Nd_{0.5}Sr_{0.5}MnO_3$ [4] is similar to that of $Pr_{0.5}Sr_{0.5}MnO_3$. However, there are few data concerning the crystal structure, magnetic and transport properties of $R_{0.5}Sr_{0.5}MnO_3$ compounds with R cations smaller than the Nd ion [8, 9]. It is demonstrated [8] that increasing the Sm content in the $(Nd_{1-y}Sm_y)_{0.5}Sr_{0.5}MnO_3$ system leads to the decreasing of the Curie temperature and suppression of charge ordering. Thus, in the compound $y = 0.875$ the ferromagnetic metallic state below $T_C = 115$ K appears to persist down to zero temperature and there is no trace of the transition to the

0953-8984/97/357455+07$19.50  

antiferromagnetic charge-ordered state at lower temperatures. Meanwhile, $Eu_{0.58}Sr_{0.42}MnO_3$ is a spin-glass insulator, that reveals a transition to the ferromagnetic metallic state in an applied magnetic field [9]. The purpose of the present study is to show how the properties of $R_{0.5}Sr_{0.5}MnO_3$ change with decreasing radii of R cations.

## 2. Experimental details

The polycrystalline samples of $R_{0.5}Sr_{0.5}MnO_{3-\gamma}$ (R = Nd, Sm, Eu, Gd, Tb, Dy, Y) were obtained by firing stoichiometric quantities of dry $R_2O_3$, $SrCO_3$ and $Mn_2O_3$ in alumina boats in air at 1710 K for 2 h after prefiring at 1170 K. $Bi_{1-x}Sr_xMnO_3$ ($0.3 \leqslant x \leqslant 0.7$) was synthesized at 1170–1470 K. All the samples were cooled slowly (100 K $h^{-1}$) to room temperature. The $Eu_{0.5}Sr_{0.5}MnO_{3-\gamma}$ sample has been prepared also using the floating zone method.

X-ray powder diffraction patterns confirm a single phase indexed on the base of the perovskite structure. No secondary phases were detected in our x-ray system which allows us to detect 2% of impurity. The oxygen content was analysed using standard redox titration. Magnetic measurements were carried out between 4.2 and 280 K with a commercial vibrating sample magnetometer. The resistance measurements were performed by the standard four-probe method. The magnetic field was provided by a 120 kOe superconducting coil. The Young's modulus has been measured using the resonance method.

## 3. Results and discussion

The nearly stoichiometric sample $Nd_{0.5}Sr_{0.5}MnO_{3-\gamma}$ ($\gamma < 0.02$) has the orthorhombically distorted perovskite structure (table 1). It shows a transition from paramagnetic insulator to ferromagnetic metal at 260 K and then to an antiferromagnetic insulating state at nearly 160 K, in correspondence with recent investigations [4, 8].

**Table 1.** Symmetry, the unit cell parameters (obtained with error ±0.001 Å), magnetic state, charge ordering temperature $T_{CO}$, Curie temperature $T_C$ (spin-glass freezing temperatures $T_f$), Néel temperature $T_N$, and off-stoichiometry oxygen content $\gamma$ of the $R_{0.5}Sr_{0.5}MnO_{3-\gamma}$ perovskites. O—orthorhombic, C—pseudo-cubic, T—tetragonal, AF—antiferromagnetic, F—ferromagnetic, SG—spin glass.

| Composition | Sym. | $a$ (Å) | $b$ (Å) | $c$ (Å) | $V$[a] (Å$^3$) | Magnetic state | $T_{CO}$ (K) | $T_C$ ($T_f$) (K) | $T_N$ (K) | $\gamma$[b] |
|---|---|---|---|---|---|---|---|---|---|---|
| $Pr_{0.5}Sr_{0.5}MnO_3$ [c] | O | 5.443 | 5.423 | 7.644 | 56.41 | AF↔F | 140 | 270 | 140 | |
| $Nd_{0.5}Sr_{0.5}MnO_{3-\gamma}$ | O | 5.435 | 5.468 | 7.630 | 56.69 | AF↔F | 150 | 260 | 150 | < 0.02 |
| $Sm_{0.5}Sr_{0.5}MnO_{3-\gamma}$ | C | 3.839 | | | 56.58 | F | | 125 | | 0.03 |
| $Eu_{0.5}Sr_{0.5}MnO_{3-\gamma}$ | C | 3.831 | | | 56.23 | SG | | 46 | | 0.04 |
| $Gd_{0.5}Sr_{0.5}MnO_{3-\gamma}$ | C | 3.830 | | | 56.18 | SG | | 44 | | 0.05 |
| $Tb_{0.5}Sr_{0.5}MnO_{3-\gamma}$ | C | 3.828 | | | 56.10 | SG | | 36 | | 0.06 |
| $Dy_{0.5}Sr_{0.5}MnO_{3-\gamma}$ | C | 3.824 | | | 55.92 | SG | | 35 | | 0.06 |
| $Y_{0.5}Sr_{0.5}MnO_{3-\gamma}$ | C | 3.821 | | | 55.80 | SG | | 35 | | 0.06 |
| $Bi_{0.5}Sr_{0.5}MnO_3$ | T | 3.906 | | 3.789 | 57.80 | AF | 540 | | 130 | |

[a] For orthorhombic unit cells $V/4$ values are given, i.e. volumes per formula unit.
[b] The values of $\gamma$ were determined with error ±0.02.
[c] Data taken from [3] and [7].

The $R_{0.5}Sr_{0.5}MnO_{3-\gamma}$ (R = Sm, Eu, Gd, Tb, Dy, Y) samples have the pseudo-cubic perovskite structure with very small unit-cell distortions at room temperature (table 1).

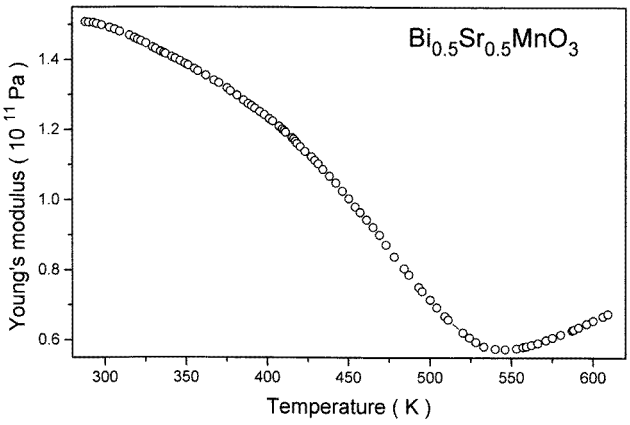


**Figure 1.** Temperature dependence of the Young's modulus of $Bi_{0.5}Sr_{0.5}MnO_3$.

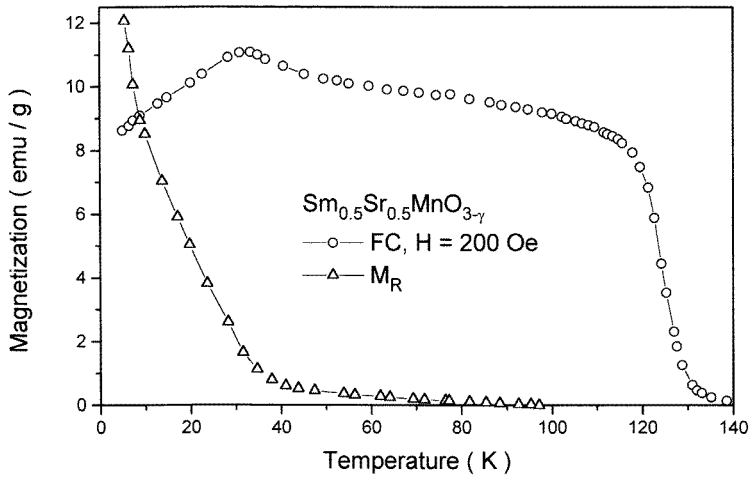


**Figure 2.** Temperature dependence of the field-cooled magnetization at 200 Oe (FC) and residual magnetization ($M_R$) of $Sm_{0.5}Sr_{0.5}MnO_{3-\gamma}$.

The absence of superstructure peaks shows indistinct $Mn^{3+}$ and $Mn^{4+}$ positions indicating a homogeneous mixed-valence state for the manganese ions. It is important to note that decrease of rare-earth ionic radii does not lead to a decrease of unit-cell volume, which can be expected on the basis of difference of radii values. The $Eu_{0.5}Sr_{0.5}MnO_{3-\gamma}$ and $Y_{0.5}Sr_{0.5}MnO_{3-\gamma}$ compounds have close unit-cell volume in spite of the relatively large difference of the ionic radii of $Eu^{3+}$ and $Y^{3+}$ (table 1). The chemical analysis of $R_{0.5}Sr_{0.5}MnO_{3-\gamma}$ (R = Sm, Eu, Gd, Tb, Dy, Y) indicates deviation from ideal stoichiometry (table 1). The most likely stabilizing cubic structure results from the emergence of the oxygen vacancies.

$Bi_{0.5}Sr_{0.5}MnO_3$ is tetragonal at room temperature. It shows a transition to cubic perovskite structure at nearly 540 K (figure 1). It is important to note that the crystal structure distortions of tetragonal $Bi_{0.4}Sr_{0.6}MnO_3$ and $Bi_{0.6}Sr_{0.4}MnO_3$ ($c/a = 0.976$ and 0.982 respectively) are less than those for $Bi_{0.5}Sr_{0.5}MnO_3$ ($c/a = 0.970$). This fact indicates

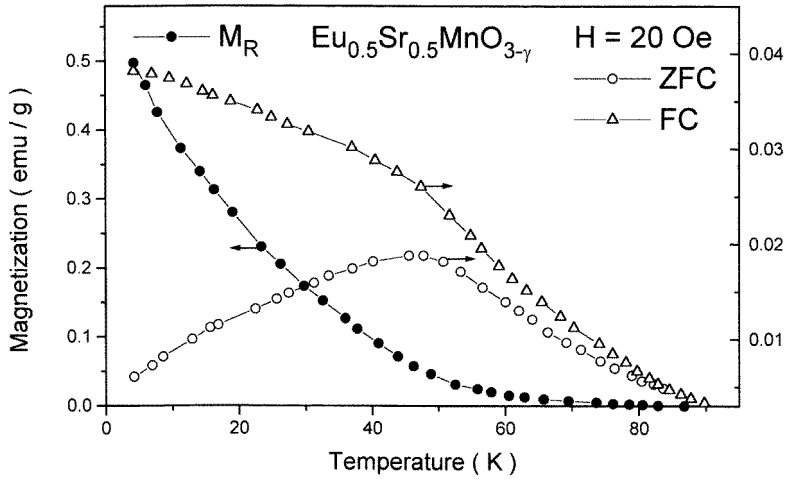


**Figure 3.** Zero-field-cooled magnetization (ZFC), field-cooled magnetization (FC) at $H = 20$ Oe and residual magnetization ($M_R$) of $Eu_{0.5}Sr_{0.5}MnO_{3-\gamma}$.

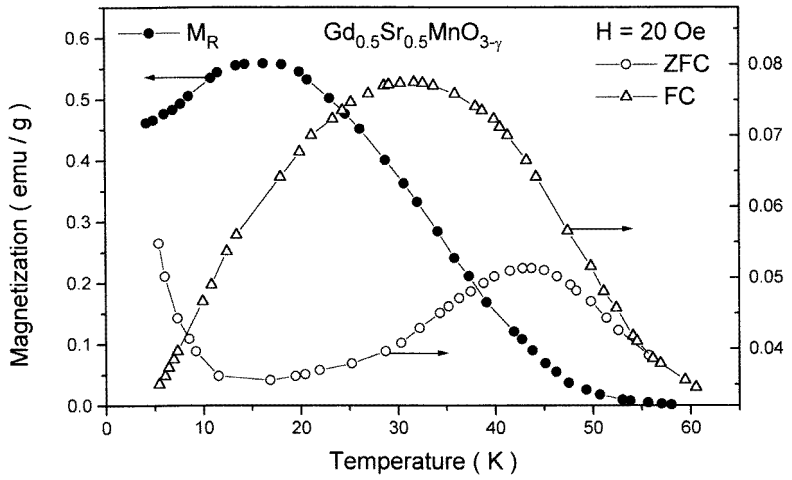


**Figure 4.** Zero-field-cooled magnetization (ZFC), field-cooled magnetization (FC) at $H = 20$ Oe and residual magnetization ($M_R$) of $Gd_{0.5}Sr_{0.5}MnO_{3-\gamma}$.

ordering of $Mn^{3+}$ and $Mn^{4+}$ ions in the ratio 1:1.

The results of magnetization measurements as a function of temperature for the $R_{0.5}Sr_{0.5}MnO_{3-\gamma}$ (R = Sm, Eu, Gd) compounds are shown in figures 2–4. The magnetization behaviour allows one to distinguish two different regions depending on the R cation. The magnetization curve of $Sm_{0.5}Sr_{0.5}MnO_{3-\gamma}$ shows a sharp jump at around 125 K corresponding to the ferromagnetic–paramagnetic phase transition (figure 2). Below 30 K the field magnetization decreases with decreasing temperature. We think that such a behaviour can arise from the samarium sublattice contribution. The fall of residual magnetization ($M_R$) below 30 K is associated with changes of magnetic anisotropy at low temperature. It was established that magnetic properties of the Eu-containing sample depend

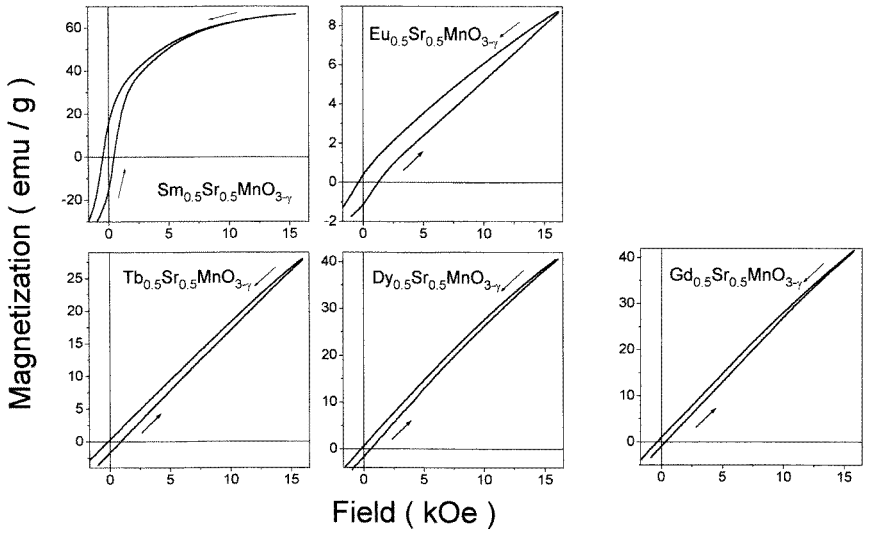


**Figure 5.** Magnetization–field data for the $R_{0.5}Sr_{0.5}MnO_{3-\gamma}$ series taken at 4.2 K.

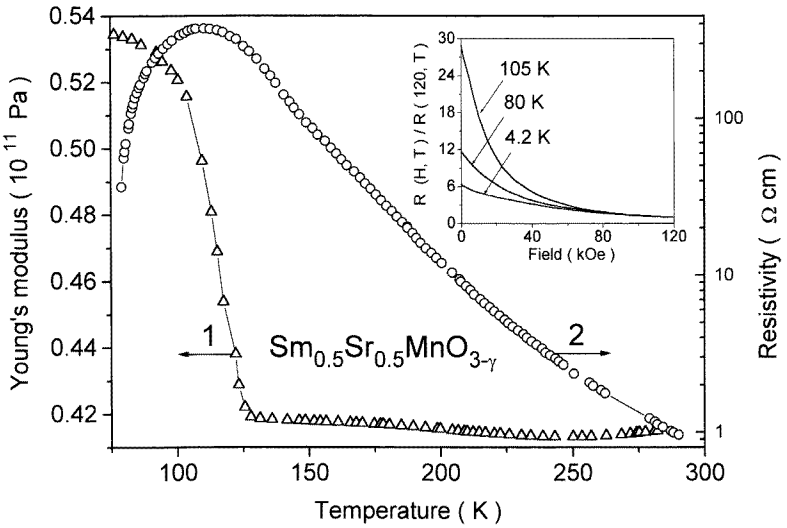


**Figure 6.** Temperature dependence of the Young's modulus and resistivity of $Sm_{0.5}Sr_{0.5}MnO_{3-\gamma}$. Inset shows magnetoresistance ratio ($MR(T) = R(H, T)/R(120\ \text{kOe}, T)$) at different temperatures.

weakly on the method of preparation. In $Eu_{0.5}Sr_{0.5}MnO_{3-\gamma}$ the jump of the magnetization disappears and a peak of zero-field-cooled magnetization (ZFC) appears at around 46 K (figure 3). Zero-field-cooled and field-cooled (FC) magnetizations do not coincide below 80 K. Such a behaviour can arise from ferromagnetic clusters in the paramagnetic (antiferromagnetic) matrix. Magnetic moments of clusters are gradually blocked with decreasing temperature. The measurements of $M$–$H$ data for $Eu_{0.5}Sr_{0.5}MnO_{3-\gamma}$ (figure 5) indicate also the absence of long-range magnetic order. Magnetization–temperature curves

for $Gd_{0.5}Sr_{0.5}MnO_{3-\gamma}$ are displayed in figure 4. ZFC and FC magnetizations show peaks at around 44 K and 33 K respectively. Below 10 K residual magnetization increases whereas zero-field magnetization falls with increasing temperature. The low-temperature behaviour can be attributed to the Gd sublattice contribution. At low temperature magnetic moments of Gd ions in ferromagnetic clusters are ordered due to negative f–d exchange interaction. The magnetic behaviour of $R_{0.5}Sr_{0.5}MnO_{3-\gamma}$ (R = Tb, Dy, Y) compounds (figure 5) is similar to that of the Gd-containing sample. There is no spontaneous magnetization in $Bi_{1-x}Sr_xMnO_3$ ($0.4 \leqslant x \leqslant 0.6$) manganites above 4.2 K. Therefore we have concluded that these compounds are antiferromagnets. The magnetic structure is stable in fields up to 120 kOe at 4.2 K. $Bi_{0.5}Sr_{0.5}MnO_3$ shows anomalous behaviour of the magnetic susceptibility at around $T_N = 130$ K.

The anomalous behaviour of Young's modulus of $Sm_{0.5}Sr_{0.5}MnO_{3-\gamma}$ at around the Curie temperature 125 K (figure 6) indicates strong magnetoelastic coupling. $Sm_{0.5}Sr_{0.5}MnO_{3-\gamma}$ exhibits a peak of resistivity below the Curie temperature (figure 6). At around the Curie temperature the magnetoresistance ratio is a maximum (figure 6). Eu-containing samples show a semiconducting type of resistance up to 4.2 K. The magnetoresistance increases gradually with increasing temperature.

As seen from presented results the properties of $R_{0.5}Sr_{0.5}MnO_{3-\gamma}$ (R = rare-earth ion) nominal composition change drastically with decreasing rare-earth radii (table 1). The compound with R = Nd has similar properties as $Pr_{0.5}Sr_{0.5}MnO_3$. The substitution of Nd ions for Sm ones leads to a fall of Curie temperature from 260 to 125 K and absence of charge-ordering phenomena in spite of the stabilization of the cubic structure. $R_{0.5}Sr_{0.5}MnO_{3-\gamma}$ (R = Eu, Gd, Tb, Dy, Y) exhibit spin-glass-like behaviour at low temperatures.

Two structural effects occur when Nd is replaced by Sm, Gd, Tb, Dy or Y (table 1):

(i) the appearance of cubic crystal structure,

(ii) the increase of oxygen vacancy content due to the lower ionic radii of heavy rare-earth ions.

These features as well as local crystal structure distortions due to the large difference in radii of rare-earth ion and $Sr^{2+}$ are key factors for understanding of magnetic property evolution of the $R_{0.5}Sr_{0.5}MnO_3$ (R = rare-earth ion, Y) series.

Usually magnetic and transport properties of the manganites are explained through the double exchange interaction [10, 11]. We think that the obtained data can be understood in the model of superexchange interaction via anions [12–14]. It was shown that $Mn^{3+}$–O–$Mn^{3+}$ superexchange interactions in perovskites are ferromagnetic if (i) manganese ions are located in octahedral surroundings and (ii) the Mn–O–Mn angle is close to 180°. The decreasing Mn–O–Mn angle as well as the decrease of the coordination number lead to the increase of the antiferromagnetic exchange interactions and decrease of the ferromagnetic ones [12, 13]. The dependence of the sign of exchange interaction on the coordination number of manganese ions as well as the appearance of local crystal structure distortions due to large difference in the ionic radii of $Sr^{2+}$ and heavy rare-earth ions must be the origin of the evolution of properties of $R_{0.5}Sr_{0.5}MnO_{3-\gamma}$ compounds.

## References

[1] Kusters R M, Singleton S, Keen D A, McGreevy R and Heyes W 1980 *Physica* B **155** 362
[2] Jin S, Tiefel T H, McCormack M, Fastnacht R A, Ramesh R and Chen L H 1994 *Science* **264** 413
[3] Tomioka Y, Asamitsu A, Moritomo Y, Kuwahara H and Tokura Y 1995 *Phys. Rev. Lett.* **74** 5108

[4] Kuwahara H, Tomioka Y, Asamitsu A, Moritomo Y and Tokura Y 1995 *Science* **270** 961
[5] Gang Xiao, McNiff E J, Gong G Q, Gupta A, Canedy C L and Sun J Z 1996 *Phys. Rev.* B **54** 6073
[6] Lees M R, Barrat J, Balakrishnan G, McPaul D and Yethiraj M 1995 *Phys. Rev.* B **52** R4303
[7] Knizek K, Jirak Z, Pollert E and Zounova F 1992 *J. Solid State Chem.* **100** 292
[8] Tokura Y, Kuwahara H, Moritomo Y, Tomioka Y and Asamitsu A 1996 *Phys. Rev. Lett.* **76** 3184
[9] Sundaresan A, Maignan A and Raveau B 1997 *Phys. Rev*. B **55** 5596
[10] Zener C 1951 *Phys. Rev.* **82** 403
[11] de Gennes P G 1960 *Phys. Rev.* **118** 141
[12] Goodenough J B, Wold A and Arnott R J 1961 *Phys. Rev.* **124** 373
[13] Havinga E E 1966 *Philips Res. Rep.* **21** 432
[14] Troyanchuk I O, Pastushonok S N, Novitskii O A and Pavlov V I 1993 *J. Magn. Magn. Mater.* **124** 55